Climate forcing of unprecedented intense-hurricane activity in the last 2000 years

Jeffrey P. Donnelly[1], Andrea D. Hawkes[2], Philip Lane[3], Dana MacDonald[4], Bryan N. Shuman[5], Michael R. Toomey[6], Peter J. van Hengstum[7], and Jonathan D. Woodruff[8]

[1]Coastal Systems Group, Department of Geology and Geophysics, Woods Hole Oceanographic Institution, Woods Hole, Massachusetts, USA, [2]Department of Geography and Geology, Center for Marine Science, University of North Carolina Wilmington, Wilmington, North Carolina, USA, [3]Deceased 11 July 2012., [4]Department of Geosciences, University of Massachusetts, Amherst, Massachusetts, USA, [5]Department of Geology & Geophysics, University of Wyoming, Laramie, Wyoming, USA, [6]The University of Texas at Austin, Jackson School of Geosciences, Austin, Texas, USA, [7]Department of Marine Sciences, Texas A&M University at Galveston, Galveston, Texas, USA, [8]Department of Geosciences, University of Massachusetts, Amherst, Massachusetts, USA

Abstract How climate controls hurricane variability has critical implications for society is not well understood. In part, our understanding is hampered by the short and incomplete observational hurricane record. Here we present a synthesis of intense-hurricane activity from the western North Atlantic over the past two millennia, which is supported by a new, exceptionally well-resolved record from Salt Pond, Massachusetts (USA). At Salt Pond, three coarse grained event beds deposited in the historical interval are consistent with severe hurricanes in 1991 (Bob), 1675, and 1635 C.E., and provide modern analogs for 32 other prehistoric event beds. Two intervals of heightened frequency of event bed deposition between 1400 and 1675 C.E. (10 events) and 150 and 1150 C.E. (23 events), represent the local expression of coherent regional patterns in intense-hurricane–induced event beds. Our synthesis indicates that much of the western North Atlantic appears to have been active between 250 and 1150 C.E., with high levels of activity persisting in the Caribbean and Gulf of Mexico until 1400 C.E. This interval was one with relatively warm sea surface temperatures (SSTs) in the main development region (MDR). A shift in activity to the North American east coast occurred ca. 1400 C.E., with more frequent severe hurricane strikes recorded from The Bahamas to New England between 1400 and 1675 C.E. A warm SST anomaly along the western North Atlantic, rather than within the MDR, likely contributed to the later active interval being restricted to the east coast.

1. Introduction

Climate controls the characteristics of tropical cyclone populations by providing the environmental conditions that influence their genesis, intensity, and path [*Emanuel et al.*, 2004; *Gray*, 1968; *Kossin and Vimont*, 2007]. Resolving how climate and tropical cyclone activity co-evolve has critical implications for society and is poorly understood. A link between human-induced climate warming and intense tropical cyclones has been suggested [*Emanuel*, 2005; *Webster et al.*, 2005], but an alternative view proposes that the recent increase in the frequency of North Atlantic tropical cyclones (Atlantic tropical cyclones with sustained winds exceeding 33 m/s are referred to as hurricanes) is related to natural oscillations in sea surface temperature (SST) [*Goldenberg et al.*, 2001]. However, the short duration and unreliability of the observational record [*Landsea et al.*, 2006] has made testing these hypotheses challenging.

Significant disagreement exists between model projections for how Atlantic hurricane activity will respond to future anthropogenic forcing, though there is some consensus that hurricane intensity will increase [*Knutson et al.*, 2010; *Villarini and Vecchi*, 2013]. Downscaling approaches indicate that warming SST may cause both more frequent and intense hurricanes in the western North Atlantic over the coming decades [*Bender et al.*, 2010; *Emanuel*, 2013]. Unfortunately, little is known regarding the sensitivity of past variability in hurricane activity to changing SST due to the limited observational record.

Coarse-grained, storm-induced deposits preserved in coastal lakes and marshes [*Boldt et al.*, 2010; *Brandon et al.*, 2013; *Donnelly and Woodruff*, 2007; *Lane et al.*, 2011; *van Hengstum et al.*, 2013; *Wallace et al.*, 2014] provide a means to extend our observational knowledge to climate regimes outside of those observed

historically, and potentially provide analogs for future climate scenarios. However, modest sedimentation rates at these sites (often less than 1 mm/year) can limit the temporal resolution of many paleo-hurricane archives. Further, challenges emerge because insufficient fine-grained sediment deposition between consecutive storm layers preclude delineation of individual events, or subsequent overwash events erode and re-work previously deposited sedimentary material [*Woodruff et al.*, 2008a]. Thus, the number of discrete storm deposits within these low-resolution records likely under-represents the total number of intense-hurricane events affecting the site.

Fortunately, a new array of high-resolution sedimentary proxy records from deep coastal basins with high sedimentation rates and low potential for post-depositional reworking are transforming our ability to detect individual hurricane-induced event beds and analyze the underlying climatic forcing of changes in hurricane activity over the last several millennia [*Brandon et al.*, 2013; *Denommee et al.*, 2014; *Lane et al.*, 2011; *van Hengstum et al.*, 2013]. Determining the spatial and temporal pattern of this past hurricane activity, and the climatic forcing mechanisms responsible for modulating intense-hurricane landfalls, is critical to assess our future risk because these past hurricane patterns may be analogs for future climate scenarios.

In this work we present a near annually resolved 2000 year record of intense-hurricane–related event beds preserved within the sediment recovered from a coastal pond (Salt Pond) in Falmouth, MA, USA (Figure 1). In combination with other previously published reconstructions from the western North Atlantic, we assess geographic patterns of intense-hurricane activity and associated climate forcings. We find that regional changes in North Atlantic SST contributed to historically unprecedented levels of intense-hurricane activity. Warm SST throughout the main development region (MDR; Figure 1a) contributed to high levels of intense-hurricane activity across the western North Atlantic for much of the first millennium Common Era (C.E.). Later, a warm SST anomaly in the western North Atlantic at the onset of the Little Ice Age (ca. 1400–1675 C.E.), coincident with a southerly shift in the Intertropical Convergence Zone (ITCZ) potentially leading to increased hurricane genesis off the southeast coast of the United States, likely contributed to an active interval of intense-hurricane activity restricted to the North American east coast, when sites in the Caribbean and Gulf of Mexico experienced low levels of intense-hurricane activity. The correspondence of active intense-hurricane regimes with regional warm sea-surface temperature anomalies,lends support to model projections of future increases in hurricane intensity associated with sea-surface warming related to greenhouse-gas emissions.

2. Methods

2.1. Study Site and Field Methods

The site of our newly developed reconstruction (Salt Pond) is a brackish coastal pond connected to the ocean via a tidal inlet with a approximately 1.3–1.8 m high (above mean high water [MHW]) coastal barrier (Figure 1). Salt Pond formed from an ice block depression (kettle) in glacial outwash sediments a few hundred meters south of the Buzzards Bay recessional moraine. Salt Pond is approximately 26 ha in area and has a relatively small total catchment area of about 70 ha. The surface of the outwash plain surrounding the pond is gently sloping with a gradient of approximately 6° and there are no significant surface water and sediment inputs from the surrounding landscape into the pond. Nearly all freshwater flux is through groundwater infiltration through the stratified coarse grained outwash sediments. Mean tidal range on the open coast is approximately 0.5 m (http://tidesandcurrents.noaa.gov/), limiting the influence of stage of astronomical tide on susceptibility of the barrier to overwash during storms. We used an Edgetech 3100 Chirp subbottom sonar system with a 4–24 kHz fish floating at the water surface to map the bathymetry and sub-bottom stratigraphic architecture of Salt Pond (Supporting Information Figure S1). Core locations were based on bathymetry and sub-bottom data. Water column salinity and temperature profiles were taken with a portable YSI Castaway CTD (Supporting Information Figure S2). We collected a series of hand driven vibracores from a raft. In each case we collected a series of replicate vibracores in an effort to maximize the total sediment recovered. In addition, we collected a replicate drive between 1 and 2 m long using a 7.5 cm diameter polycarbonate piston core at each core location to ensure we recovered an intact sediment/water interface (preserving the most recent portion of the record) at each coring location.
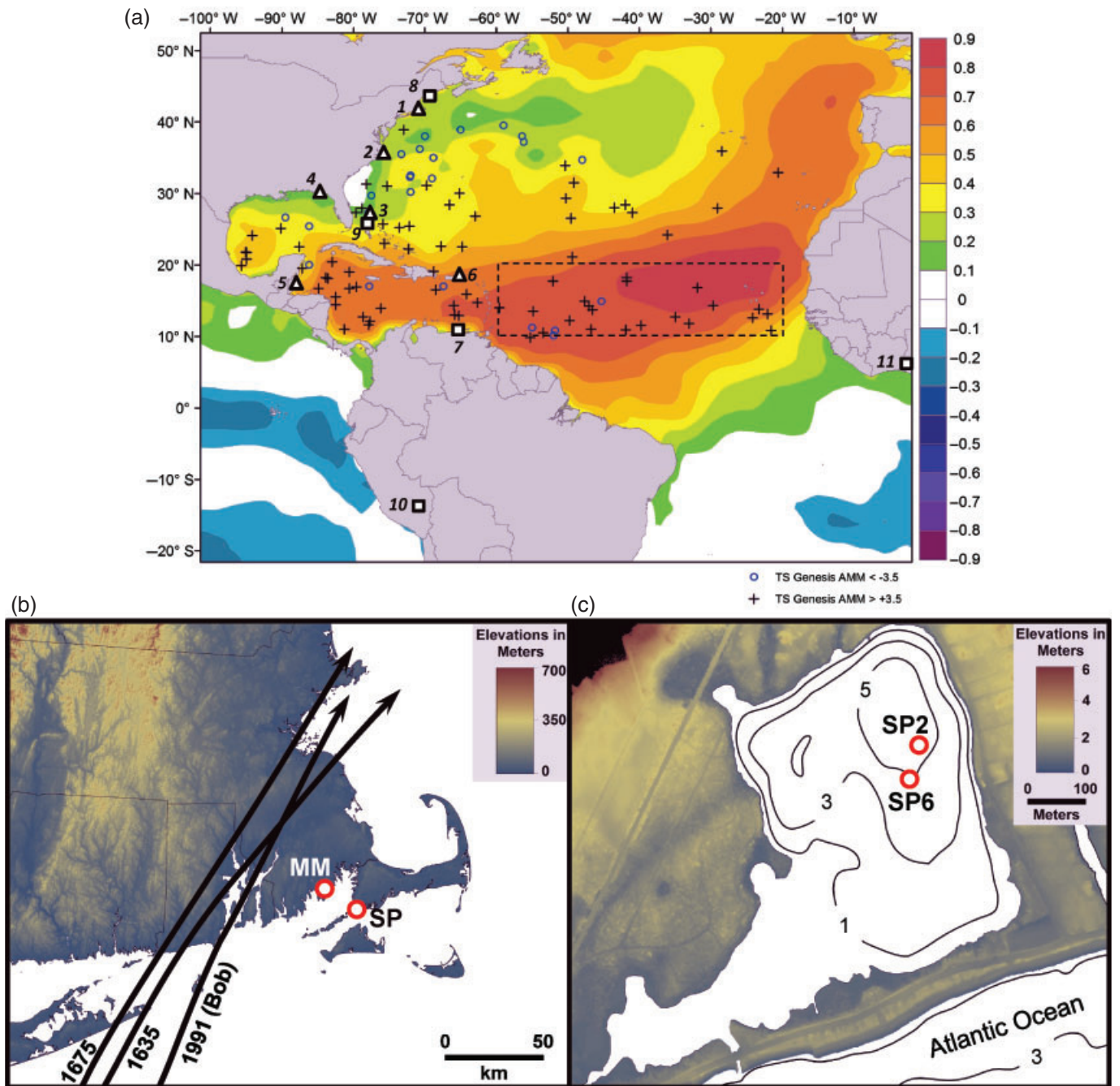
Figure 1. Location maps. (a) Correlation map of boreal summer SST and AMM. SSTs are warmer during positive AMM. Triangles show locations of paleo-hurricane reconstructions presented here (*1*—Salt Pond [this study] and Mattapoisett Marsh [*Boldt et al.*, 2010]; *2*—Outer Banks inlets [*Mallinson et al.*, 2011]; *3*—Thatchpoint Blue Hole [*van Hengstum et al.*, 2013], *4*—Mullet Pond [*Lane et al.*, 2011] and Spring Creek Pond [*Brandon et al.*, 2013]; *5*—Lighthouse Blue Hole [*Denommee et al.*, 2014]; *6*—Laguna Playa Grande [*Donnelly and Woodruff*, 2007]). The MDR for North Atlantic tropical cyclones is noted in the dashed box. Locations of additional paleoclimate proxy records presented in Figures 4 and 5 are noted with squares (*7*—Cariaco Basin [*Wurtzel et al.*, 2013; *Haug et al.*, 2001]; *8*—Gulf of Maine SST [*Wanamaker et al.*, 2008]; *9*—Bahamas SST [*Saenger et al.*, 2009]; *10*—Quelccaya Ice Cap [*Thompson et al.*, 2013]; *11*—Lake Bosumtwi [*Shanahan et al.*, 2009]). Genesis locations for hurricanes forming in the most positive AMM (+) and most negative AMM (o) years are shown. Note the increase in genesis off the North American east coast in negative AMM. (b) Location of Salt Pond (SP) and Mattapoisett Marsh (MM) [*Boldt et al.*, 2010] in southeastern New England and approximate tracks of historical hurricanes thought to have left a coarse event bed in Salt Pond sediments. (c) Map of Salt Pond showing core locations (SP2, SP6) and bathymetry and topography in meters.

2.2. Laboratory Analysis

Cores were transported to the laboratory, sectioned, split and described. Archived core halves were scanned on the ITRAX X-ray fluorescence (XRF) scanner at Woods Hole Oceanographic Institution (WHOI). X-ray radiography was measured simultaneously with elemental chemistry at 200 μm resolution. We focused our analysis on cores collected from the deepest region of the basin (i.e., SP2 and SP6; Figure 1c). In core SP2 and for the upper 50 cm of core SP6 we measured the organic content of the sediment using loss on ignition [*Dean*, 1974] (LOI) every contiguous half centimeter. Following the LOI process, we sieved the remaining ash at 32 μm and then 63 μm and dried and weighed the residual to determine the percentage of these fractions relative to the total dry weight of the sediment. Weighing errors of ±0.002 g result in percent coarse uncertainities of ±0.25% (at 95% confidence).

2.3. Chronology

We use several isotopic and stratigraphic dating methods to establish age control. The activity of ^{137}Cs within sediments provides stratigraphic markers associated with nuclear weapons testing. The beginning of ^{137}Cs deposition occurred in 1954, followed by peaks in 1959 and 1963 C.E. [*Dunphy and Dibb*, 1994]. The ^{137}Cs activity of selected subsamples from cores SP2 and SP6 were measured at WHOI using a high-resolution Canberra gamma detector.

Pollution horizons preserved in the sediments can also provide a dated stratigraphic marker. For example, lead pollution introduced to the atmosphere beginning at the onset of the industrial revolution quickly precipitated out of the atmosphere and was rendered immobile in anoxic sediments [*McCaffrey and Thomson*, 1980]. Records of lead pollution preserved in sediments can provide a stratigraphic marker that dates to the late-1800s [*Donnelly et al.*, 2001] and when lead was removed from gasoline in the 1970s and 1980s [*Wu and Boyle*, 1997; *McConnell et al.*, 2002]. We used lead levels from XRF scans to examine temporal trends in lead content of the sediment.

Regional alteration of terrestrial flora as documented by fossil pollen records also provides chronostrati-graphic markers. We took 1 cm^3 samples at 20 cm intervals (40 year resolution) throughout SP2 for pollen analysis. Samples were processed using standard techniques [*Faegri and Iverson,* 1989] and pollen was identified and counted to over 400 arboreal taxa per level. The increase of native and introduced weeds (ragweed [*Ambrosia sp.* L.] and sorrel [*Rumex sp*. L.], respectively) associated with European-style clearance in the northeastern United States is well represented by pollen data, providing a well-dated stratigraphic marker [*Russell et al*., 1993]. Opaque spherules were also identified and counted in all pollen samples, where a 1900 C.E. rise in the northeast United States has been associated with industrial activities [*Clark and Patterson*, 1985].

Terrestrial macrofossils preserved within core SP2 were dated by accelerator mass spectrometry (AMS) radiocarbon techniques at the National Ocean Sciences Accelerator Mass Spectrometer (NOSAMS) facility at WHOI (Figure 2b; Supporting Information Table S1). Radiocarbon results were calibrated for secular changes in atmospheric radiocarbon concentrations (IntCal13 [*Reimer et al.*, 2013]). Age models and associated 95% uncertainties were computed using BACON (Bayesian accumulation histories for deposits) software [*Blaauw and Christen*, 2011] for SP2 and previously published sites used for comparison: Thatch-point Bluehole [*van Hengstum et al.*, 2013], Laguna Playa Grande, Vieques [*Donnelly and Woodruff*, 2007], and the Cariaco Basin SST record [*Wurtzel et al.*, 2013; from original radiocarbon results in *Black et al.,* 1999]. Thus, the age models for Thatchpoint and Vieques are updated from the originally published versions (Supporting Information Figure S3), which were simple linear interpolated segments between dated index points.

2.4. Determining Event Bed Threshold

In order to determine a cutoff for what constitutes an event bed at Salt Pond we calculated the cumulative distribution of coarse fraction that exceeded 99% of the data over the historical interval in core SP2 (last 393 years), or 1.34%. In turn, we define events over the entirety of the 2000 year SP2 record based on those coarse fraction peaks that exceed 1.34% coarse fraction (Figure 2a). In order to filter out the multiyear to decadal variability in coarse fraction, we subtract an 11-point moving average from the data that excludes coarse fraction values that exceed 5%. By excluding the large peaks in coarse fraction from the moving average, we prevent the filter from screening coarse fraction peaks
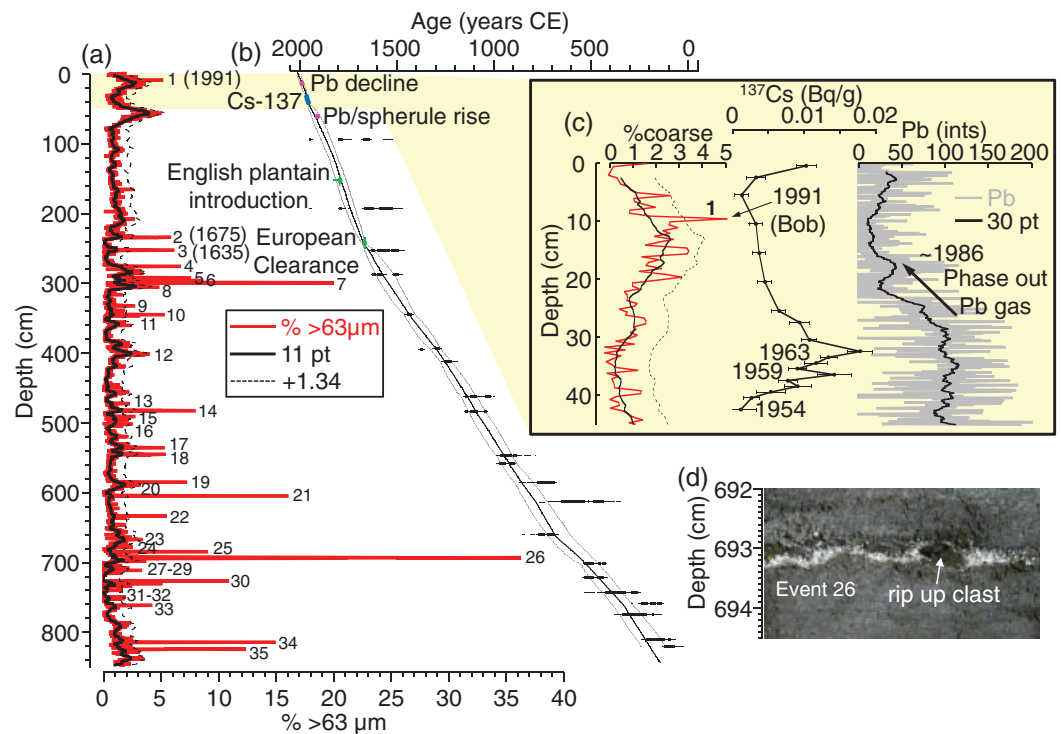
Figure 2. Overwash event record from Salt Pond, MA. (a) Percent sand fraction (>63 µm) results (red) from core collected from the deepest part of the basin (SP2) with 11-point running mean filter that excludes coarse fraction values exceeding 5% (black). Dashed line is event threshold of >1.34%. Events are numbered 1–35. (b) Age model derived from radiocarbon (2σ ranges thin bars and 1σ ranges thick bars; 95% confidence bounds shown around mean age; Supporting Information Table S1) and stratigraphic dates, including pollen evidence (green) of European land clearance and agriculture in the late seventeenth century and the introduction of English plantain in the early nineteenth century (Supporting Information Figure S5). [137]Cs activity provides ages related to nuclear weapons testing in the middle twentieth century (blue). Pb pollution and opaque spherules provide ages related to industrialization (purple). (c) Blow up of the upper 45 cm of percent sand fraction data with ^{137}Cs and bulk Pb pollution chrono-horizons. The event bed attributed to Hurricane Bob is noted. This portion of the record is replicated in core SP6 (Supporting Information Figure S6). (d) Photograph of event bed 26 at 693 cm.

adjacent to large peaks in coarse fraction that in other parts of our record would be well above our event threshold of 1.34%.

2.5. Determining Event Frequency

We follow the approach by *Lane et al.* [2011] and generate an event frequency per 100 years for the SP2 record by applying a sliding 162 year window, the same duration of the historic best-track data set, through the event data. This facilitates comparisons between storm frequency in the instrumental record (1851–2013 C.E.) and event frequency in the paleorecord. Moving averages of event frequency were obtained using the average occurrence rate of significant coarse fraction anomalies per year within the sliding 162 year window.

The frequency plot for Mullet Pond follows that originally published by *Lane et al.* [2011]. However, the frequency plot for Spring Creek Pond [*Brandon et al.*, 2013] was created by applying a D90 threshold of 325 µm for defining intense-hurricane event beds (roughly equivalent to modeled category 3 intensity) and then applying the 162 year moving window as above. For the Laguna Playa Grande record from Vieques (LPG4) [*Donnelly and Woodruff*, 2007], a 31-point moving average was subtracted from the data to filter out long-term variations in mean grain size and then we applied a threshold of 12 µm for event beds. A moving average of event frequency was obtained using the average occurrence rate of significant coarse fraction anomalies per year within the sliding 162 year window as above. For the Lighthouse Bluehole [*Denommee et al.*, 2014] frequency plot we converted the events per 20 year data provided by Denommee et al. to events per century with a 162 year moving average.

2.6. Calculating Expected Frequency Based on Observational Record

To calculate an estimate of modern return rate (λ) for the Salt Pond Site we used the frequency of category 2 or greater hurricanes in the northeastern United States over the past 162 years (the interval of the NOAA Best Track dataset), which is the approximate threshold event based on historic event bed deposition (see results below). Seven events with sustained winds over 43 m/s ($\geq$CAT 2 intensity) made landfall in southern New England since 1851 C.E. (Supporting Information Figure S4) resulting in a probability of 4 storms per century for the entire southern New England coast. The maximum impact from surge and waves is typically felt within the radius of maximum winds to the east of the storm track in New England as the storms translate northwards. As a result we divide the 325 km of southern New England by the mean radius of maximum winds at this latitude of 65 km [*Boldt et al.*, 2010; *Kossin et al.*, 2007] and divide the probability of a category 2 or greater landfall in southern New England by that value. Thus, λ = ([7 events/162 years]*100)/[325 km/65 km] = 0.9 events per century/65 km of the southern New England coast. Implicit in this estimate is the assumption that the probability of a category 2 or greater hurricane strike is equal along the entire southern New England coast.

As a result of the stochastic nature of hurricane landfalls, the number of storms impacting a specific site might vary from one sampled period to the next even if the statistics of Atlantic hurricanes were stationary through time. Thus, some portion of the variability in local flooding frequency may be due to chance alone, while the remainder may have resulted from actual changes in hurricane climate. We calculate the cumulative Poisson probability (P) of equaling or exceeding 0, 1, 2, 3, 4, and 5 events per century (X) given the expected probability (λ):

$$P(x, \lambda) = 1 - \sum_{k=0}^{x} \frac{e^{-\lambda} \lambda^k}{k!}$$

3. Results and Discussion

3.1. Salt Pond Reconstruction

3.1.1. Event Beds and Chronology

The 5.5 m deep basin in the northeast corner of Salt Pond, about 400 m from the current shoreline (Figure 1), has rapidly filled with sediment over the last two millennia (sedimentation rates between 4 and 7 mm/year; Figure 2). Core SP2 is 840 cm long and numerous quartz sand (>63 μm) event beds punctuate the otherwise fine-grained, organic-rich sediments (Figures 2a and 2d). Salinity stratification (Supporting Information Figure S2) results in anoxic bottom water preserving annual laminations throughout much of the archive. As described above, we define event beds as those coarse fraction peaks that exceed 99% of the cumulative distribution of coarse fraction over the historical interval (last 393 years), or >1.34% coarse fraction (Figure 2a). Based on this criterion we identify 35 event beds in core SP2 (Figure 2a).

A combination of radiocarbon dates on plant macrofossils and chronostratigraphic markers provide age control for core SP2 (Figure 2b). We interpret the increase in total herbs and the appearance of cereal rye (*Secale cereal* L.) pollen in the record at 235–236 cm in SP2 as the onset of European land clearance and agriculture in the late 1660s and 1670s [*Geoffrey*, 1930] (Figure 2b; Supporting Information Figure S5). The appearance of English plantain (*Plantago lanceolata* L.) pollen at 144–145 cm provides evidence of the introduction of this non-native species in the first half of the nineteenth century (1800–1850 C.E.) [*Clark and Patterson*, 1985]. The dramatic increase in opaque spherules at 59–60 cm (Figure 2b; Supporting Information Figure S5) is coincident with the rise in lead pollution and likely dates to the industrial revolution in the late 19th and early 20th centuries [*Donnelly et al.*, 2001]. [137]Cs activity provides dated markers associated with nuclear weapon testing [*Dunphy and Dibb*, 1994] with the initial rise at 39.5 cm dating to 1954 C.E., and peaks in activity at 36.5 and 32.5 cm dating to 1959 and 1963 C.E., respectively (Figure 2c). The decrease in lead levels that occurs between approximately 28 and 18 cm (Figure 2c) is diagnostic of reduced lead accumulation related to its removal from gasoline in the 1970s and 1980s [*Wu and Boyle*, 1997].

3.1.2. Event Attribution

The most recently deposited coarse-grained event bed (#1) occurs at about 10 cm depth and based on our age model dates to between 1982 and 2005 C.E. at 95% confidence (Figures 2b and 2c; Supporting Information Figure S6). This event bed was likely deposited by Hurricane Bob in 1991 C.E., the only category 2 or greater storm since 1851 C.E. [*Landsea et al.*, 2004] to pass within 100 km to the west of Falmouth (Supporting Information Figure S4). Hurricane Bob passed about 60 km west of Salt Pond (Figure 1b) with maximum sustained winds of 45 m/s, causing a storm tide approximately 1.6 m above MHW in Falmouth [*Boldt et al.*, 2010] and maximum offshore wave heights of approximately 4 m [*Cheung et al.*, 2007]. Washover fans across the western portion of the barrier fronting Salt Pond evident in aerial photographs taken immediately following Hurricane Bob indicate overtopping by the combination of surge and wave runup (Supporting Information Figure S7). Historically, severe winter storms and tropical cyclones that either pass offshore or make landfall to the east have failed to produce storm tides capable of overtopping the barrier fronting Salt Pond (see Supporting Information) [*Boldt et al.*, 2010]. Conversely, hurricanes that made landfall further west than Bob in the middle part of the twentieth century (e.g., 1938, 1944 C.E.) produced storm tides capable of overtopping the Salt Pond barrier [*Boldt et al.*, 2010], yet these events did not leave coarse event bed in Salt Pond. The lack of distinct event beds related to these more distal hurricane strikes suggests that local wind speeds in Falmouth were insufficient to generate waves large enough to transport sediment the more than 400 m to the deep basin in the northeast corner of Salt Pond. For example, 1-min sustained wind speeds associated with the 1938 Hurricane at Edgartown, 20 km southeast of Salt Pond, were only 33 m/s [*Brown*, 1939] (using a conversion factor of 1.07 from 5-min to 1-min sustained winds). Similarly, the closest maximum sustained wind observation for the 1944 hurricane of 27 m/s comes from Nantucket (57 km to the southeast of Salt Pond) [*Sumner*, 1944]. In contrast, maximum sustained winds in Falmouth during Hurricane Bob were measured at 38 m/s, with gusts reaching 56 m/s [*Mayfield*, 1991].

Deeper in core SP2, two event beds at 253 and 235 cm depth, date to 1614–1660 C.E. (mean = 1639 C.E.) and 1668–1695 C.E. (mean = 1679 C.E.) at 95% confidence, respectively (Supporting Information Figure S5). These event beds were most likely deposited by well-documented severe hurricane strikes in 1635 and 1675 C.E. [*Ludlum*, 1963]. The first of these is the Great Colonial Hurricane of 25 August 1635, which passed across southeastern New England and caused widespread damage consistent with a category 3 hurricane [*Boose et al.*, 2001]. Hindcast surge modeling indicates surge likely reached about 3.5 m at Salt Pond [*Boldt et al.*, 2010]. Both the track and impact of the 1675 (7 September) hurricane were similar to the Great Colonial Hurricane of 1635 in southeastern New England [*Ludlum*, 1963].

The hurricane-induced event beds preserved in the historic sediments at Salt Pond indicate a similar frequency of severe hurricane impacts compared to those derived from our approach using the Best Track data that we discuss above. Specifically, three events in 393 years (1620–2013 C.E.) yields a frequency of 0.8 events per century compared to a value of 0.9 events per century derived from the approach using category 2 or stronger storms making landfall in all of southern New England since 1851 C.E. and dividing by the mean radius of maximum winds.

3.1.3. Changes in Event Frequency

The Salt Pond record indicates considerable changes in the frequency of event beds over the last 2000 years, with historically unprecedented intervals of event-bed deposition. A total of 35 event layers were deposited over the last 2000 years (Figures 2a and 3a); the highest frequencies were reached at 1420–1675 C.E. (10 event beds, #2–11) and 150–1150 C.E. (23 event beds, #13–35). Assuming hurricane landfall occurrence follows a Poisson process we can estimate the probability of exceeding the number of events expected by random chance alone. For example, using 0.9 events per century as the expected rate (λ) (derived from the 162 year NOAA Best Track Dataset, Supporting Information Figure S4), the probability of experiencing three or more events in any one century is 0.06 (6%). Several intervals in the 4–7th centuries, eleventh century, and 15th to early 17th centuries exceed this frequency (Figure 3a). The probability of experiencing one or more events in any one century is 0.6 (60%). However, the probability of experiencing 10 consecutive centuries with one or more events per century, as recorded at Salt Pond between ca. 150 and 1150 C.E., is quite low at 0.006 (0.6%). Similarly, the probability of experiencing two or more events in two consecutive centuries, as reconstructed in Salt Pond between ca. 1440 and

1640 C.E. (Figure 3a), is only 0.04 (4%), and in fact event bed frequency exceeds three events per century through most of this interval. Hence, compared to modern event frequencies in the region, significant portions of the 2000 year Salt Pond record exceed what would be expected based on random event occurrence alone.

3.1.4. Event Intensity

Given that sedimentary archives only preserve evidence of events that exceed the local intensity threshold necessary to transport and deposit coarse grained material to sediment depo-centers, archives such as Salt Pond are likely to record the passage of more intense storms. As a result, the temporal patterns in event bed deposition may reflect changes in the frequency of only the more intense storms that are capable of producing event beds. The populations of storms that can locally produce event deposits likely have varying characteristics (e.g., track, intensity, size) [*Lin et al.*, 2014]. In the case of Salt Pond, less intense historical events (minor tropical cyclones, extratropical storms, and more distal intense storms) have been unable to generate local surge, wave heights and currents sufficient to transport sand-sized material more than 400 m from the barrier to the location of SP2. The last 350 years of sediment accumulation at Salt Pond indicates that only relatively intense hurricanes making a close landfall (~100 km) to the west of the site have left event beds. Given modest increases in sea level over the last 2000 years in the region [*Donnelly*, 1998] (~2 m), the barrier fronting Salt Pond has likely transgressed landward with time, with recent historical shoreline retreat rates of approximately 10 m per century [*Thieler et al.*, 2013]. As a result of this landward barrier translation, older event beds recorded in SP2 were likely transported greater distances than recent ones, which may point to even greater local intensities for prehistoric events relative to Hurricane Bob in 1991 C.E.

Out of the 32 prehistoric event beds 12 beds contain more coarse sediment than that deposited by the Great Colonial Hurricane in 1635 C.E. (event bed #3), despite likely being trans-
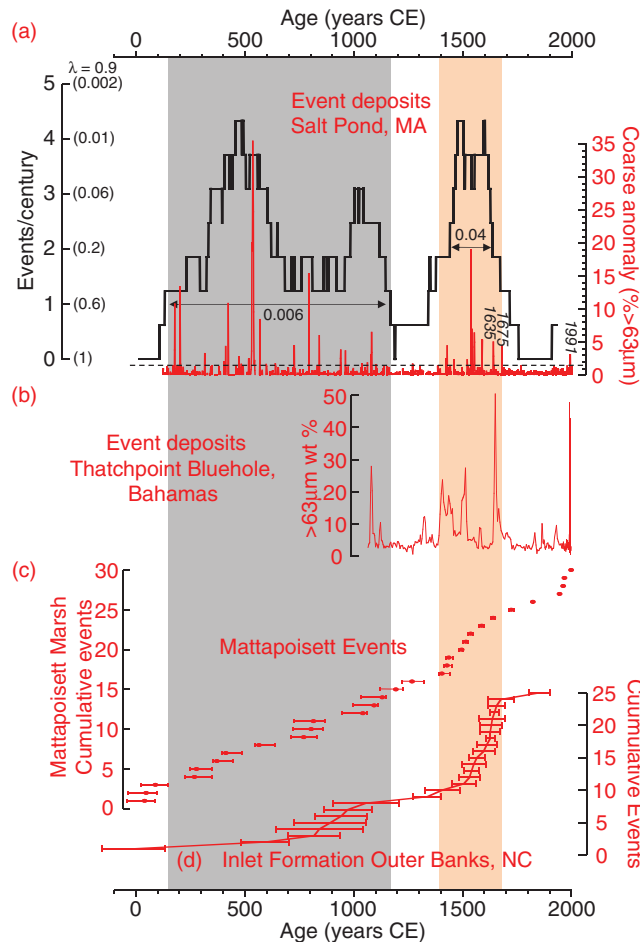

Figure 3. Comparison of hurricane proxy records from North American east coast. (a) Coarse anomaly plot from Salt Pond with event bed threshold of 1.34% coarse shown as dashed line. Historical hurricane strikes attributed to event beds are noted. Gray is event frequency with associated Poisson probabilities of occurrence assuming 0.9 events per century (i.e., modern climatology). Arrows are continuous centuries with more than 1 event per century and 2 events per century and their associated probabilities under modern climatology. (b) Event beds from a sediment core from Thatchpoint blue hole in The Bahamas [*van Hengstum et al.*, 2013]. (c) Cumulative event frequency of overwash events preserved in Mattapoisett Marsh, MA [*Boldt et al.*, 2010]. Mattapoisett Marsh is a backbarrier salt marsh 18 km to the northwest of Salt Pond. (d) Cumulative frequency plot of inlet formation from the Outer Banks of NC [*Mallinson et al.*, 2011]. Shading is intervals (150–1150 C.E. and 1400–1675 C.E.) when Salt Pond records heightened intense-hurricane–related event beds.

ported a greater distance due to barrier transgression related to sea-level rise. The largest coarse anomaly peak occurs at 693 cm (event bed #26, Figure 2) and dates to ca. 540 C.E.. A rip-up clast of fine-grained organic sediment incorporated in the ca. 540 C.E. quartz sand deposit further attests to the layers origin

from a high-energy event (Figure 2d). While the amount of coarse fraction transported is only one metric for ascertaining the local intensity of an event [*Brandon et al.*, 2013; *Woodruff et al.*, 2008b], these large coarse fraction peaks suggest that the competence of local event driven waves and currents to transport sand-sized particles was greater during recent prehistory than experienced over the last ca. 400 years. This implies that many of the prehistoric hurricanes may have locally been more intense than those impacting the region historically.

3.2. Regional Patterns

While the Salt Pond record provides only a local archive of intense-hurricane occurrence, basin-wide, or regional changes in hurricane climate can potentially be inferred by examining reconstructions from different regions [*Kozar et al.*, 2013]. One of the most active intervals at Salt Pond consists of 10 event beds between 1420 and 1675 C.E. (Figure 3a), with five of these events occurring between 1500 and 1600 C.E. Several additional lines of evidence suggest that the North American east coast (hereafter east coast) experienced heightened intense-hurricane activity at this time. Reconstructions of hurricane-induced event beds from Thatchpoint Bluehole in the Bahamas [*van Hengstum et al.*, 2013] and Mattapoisett Marsh, MA [*Boldt et al.*, 2010] reveal similar sequences of event beds attributed to hurricanes over the last millennium, with the most event beds between 1400 and 1675 C.E. (Figures 3b and 3c). Further, increased frequency of inlet formation along the Outer Banks of North Carolina [*Mallinson et al.*, 2011] (Figure 3d) and extensive erosion events in Connecticut salt marshes [*van de Plassche et al.*, 2006] between 1400 and 1675 C.E. also point to increased intense storminess.

The strong correspondence between event beds at Thatchpoint Bluehole in The Bahamas and Salt Pond further supports that the event beds at Salt Pond are related to hurricanes. Unfortunately, the record at Thatchpoint currently only extends back 1000 years, but the two events there that date to close to 1100 C.E. appear to correspond to the very end of the earlier active interval at Salt Pond (Figure 3). Mattapoisett Marsh [*Boldt et al.*, 2010] provides the closest confirmation of the period of heightened activity recorded at Salt Pond, 18 km to the southeast. Though a much lower resolution archive than Salt Pond, Mattapoisett Marsh likely records many of the same hurricane events as Salt Pond, including a cluster of eight events between 1400 and 1675 C.E. (Figure 3). In the historical period, event beds associated with hurricanes in 1991 C.E. and 1635 C.E. are recorded at both locations, unlike Salt Pond to the southeast, however, Mattapoisett Marsh also records the series of hurricane strikes that made landfall further west in Long Island NY in the mid-twentieth century (1938, 1954–Carol, 1960–Donna, 1815, 1727 C.E.). Given their close proximity and the overlapping ages of event beds at both sites, many of the same prehistoric events recorded at Salt Pond are likely also present at Mattapoisett Marsh. Similar to the historical interval, however, Mattapoisett Marsh also likely records some hurricanes making landfall further west.

Increased frequency of barrier island breaching along the Outer Banks of North Carolina provides further evidence of enhanced storminess along the east coast between 1400 and 1675 C.E. [*Mallinson et al.*, 2011] (Figure 3d). At least 15 barrier-beach breaches occurred in this interval, which is in stark contrast to the preceding and following two centuries when only one or two breaches occurred. Earlier, at least seven inlets were cut in the Outer Banks between 500 and 1100 C.E. when Salt Pond also showed heightened event bed deposition. Only one inlet breach was documented prior to 500 C.E., but the low preservation potential of older inlets as the barriers transgress landward with sea-level rise likely limited the length of this archive.

Taken together, the four different reconstructions provide evidence of a synchronous interval of heightened intense-hurricane activity along the east coast between 1400 and 1675 C.E. However, when one compares these records to reconstructions from the Gulf of Mexico (GoM) (Figures 4b and 4c) and Caribbean (Figures 4d and 4e) a more complex pattern emerges. For example, the interval between 1400 and 1675 C.E. appears to be one of relatively low intense-hurricane activity in the GoM and Caribbean, as reconstructions from Vieques [*Donnelly and Woodruff*, 2007], Belize [*Denommee et al.*, 2014], and Apalachee Bay, FL [*Brandon et al.*, 2013; *Lane et al.*, 2011] all preserve relatively few event beds at this time (Figures 4b–4e). Thus, the interval of elevated intense-hurricane activity between 1400 and 1675 C.E. appears to have been restricted to the east coast.
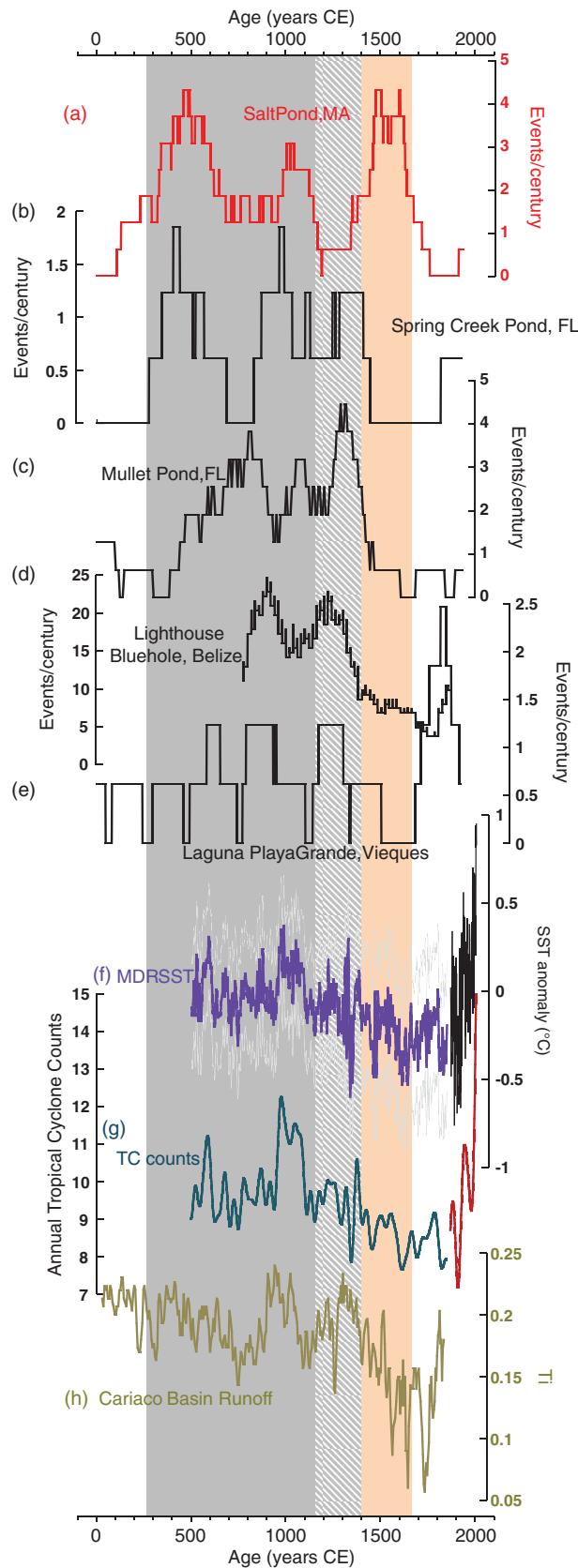
The earlier period of heightened event bed deposition at Salt Pond from 150 to 1150 C.E. is one where other overwash proxy records from the western North Atlantic also reveal frequent event bed deposition, though the timing of peaks in activity sometimes vary (Figure 4). These records suggest that the entire North Atlantic basin experienced more frequent intense-hurricane strikes over much of this interval. However, the reconstructions from the Caribbean and GoM all remain active until about 1400 C.E., while the east coast is quiescent between 1150 and 1400 C.E.. This suggests that, either storms failed to track up the east coast and/or conditions were not favorable for intense hurricanes to maintain their strength off the east coast at this time.

For example, an archive of the coarsest grained event deposits from Spring Creek Pond on the Florida Panhandle [*Brandon et al.*, 2013] indicates heightened intense-hurricane frequency between 250 and 1400 C.E., save a short interruption in the eighth century (Figure 4b). Large coarse grained deposits from nearby Mullet Pond [*Lane et al.*, 2011] are also more frequent between about 400 and 1400 C.E. (Figure 4c). A reconstruction of hurricane event beds from Lighthouse Bluehole in the western Caribbean [*Denommee et al.*, 2014] dating back to 700 C.E. also indicates higher incidence of events between 750 and 1400 C.E. relative to the last 600 years (Figure 4). Even the lower resolution Laguna Playa Grande record [*Donnelly and Woodruff*, 2007] from Vieques, Puerto Rico (Figure 4e), where storm undercounting is a significant issue due to the slow prehistoric sedimentation rate there (see discussion in [*Woodruff et al.*, 2008a]), suggests heightened intense-hurricane activity between 250 and 1400 C.E.

Like the reconstructions from Spring Creek Pond and Mullet Pond (Figure 4), the Salt Pond sediments record few intense events over the last century. Only one event is recorded at Salt Pond (Bob in 1991) during this time, however, the lack of recent event beds may simply reflect that Falmouth was relatively fortunate in

Figure 4. Legend on next page

the twentieth century and largely avoided severe hurricane impacts. In contrast, were Salt Pond located a short distance to the west (like Mattapoisett Marsh), the site would have more severely experienced three hurricane strikes in the middle of the twentieth century (e.g., 1938, 1954, and 1960) that could potentially have left event beds. Conversely, the reconstructions from Belize (Figure 4d), Vieques (Figure 4e), and The Bahamas (Figure 3b) record recent increases in event bed frequency, but interestingly the increase at Vieques appears to predate the twentieth century. With the exception of Vieques, where the identification of more event beds in the historical interval may be related to an increase in sedimentation rate [*Woodruff et al.*, 2008a], the remaining reconstructions examined here suggest the early portion of the historic interval (ca. 1700–1900 C.E.) was relatively quiescent with respect to intense hurricanes when compared to the last two millennia.

3.3. Climatic Forcing

As described above, available high-resolution and well-dated reconstructions from the western North Atlantic reveal coherent patterns of intense-hurricane activity on multi-centennial time scales over the last 2000 years. While some geographic variability exists in the timing of peaks in activity, most reconstructions indicate that much of the first millennium C.E. was more active than that experienced historically. The interval between 1150 and 1400 C.E. is one in which only the Caribbean and GoM see increased activity, while the east coast is inactive. The reconstructions from the Caribbean and GoM all see a dramatic decrease in event bed frequency around 1400 C.E., when the east coast becomes active until the late seventeenth century.

Warm SST in the MDR of the tropical North Atlantic, coincident with a more northerly position of the ITCZ, promotes cyclogenesis and potential tropical cyclone intensity in the MDR by increasing low-level vorticity, and decreasing vertical wind shear and sea-level pressure [*Kossin and Vimont*, 2007]. The relationship between Atlantic hurricane activity and warm MDR SST and northerly ITCZ position has been documented on inter-annual [*Kossin and Vimont*, 2007] (Supporting Information Figure S8) to multi-decadal timescales [*Goldenberg et al.*, 2001; *Zhang and Delworth*, 2006]. The location of the ITCZ also impacts precipitation patterns across the tropics (Supporting Information Figure S9), explaining why twentieth century rainfall in the Sahel region of Africa correlates well with hurricane activity [*Gray*, 1990]. Similar centennial-scale shifts in ITCZ position and MDR SST may explain the strong anti-correlation observed between Ecuadoran extreme precipitation [*Moy et al.*, 2002] with the coarsely resolved intense-hurricane record from Vieques, Puerto Rico over the last five millennia [*Donnelly and Woodruff*, 2007].

While high-resolution proxy reconstructions of SST directly from the MDR (Figure 1a) are limited by slow rates of pelagic sedimentation and the absence of suitable corals, statistical reconstructions based on networks of proxy data are available. The Mann et al. (hereafter M09) reconstruction of MDR SST is shown in Figure 4f and documents decadal to centennial scale variations in MDR SST over the last 1500 years [*Mann et al.*, 2009].

In modern climate, La Niña conditions typically favor increased tropical cyclone genesis in the MDR [*Kossin et al.*, 2010] and indices of MDR SST and El Niño/Southern Oscillation are good predictors of historical Atlantic hurricane trends [*Kozar et al.*, 2012]. Statistical modeling of basin-wide activity over the last 1500 years by M09, based primarily on MDR SST and Niño3 temperatures, predicts relatively higher levels of basin-wide hurricane activity between 500 and 1400 C.E. (Figure 4g), when MDR SST is relatively warm. Consistent with the M09 model result, the coastal sediment records indicate heightened

Figure 4. Comparison of Salt Pond reconstruction with Caribbean and GoM hurricane proxy records, reconstructed MDR SST, modeled hurricane activity, and Cariaco Basin runoff. (a) Event bed frequency at Salt Pond, MA (as in Figure 3). (b) Intense-hurricane event bed frequency from Spring Creek Pond, FL [*Brandon et al.*, 2013]. (c) Intense-hurricane event bed frequency from Mullet Pond, FL [*Lane et al.*, 2011]. (d) Event bed frequency from Lighthouse Bluehole, Belize [*Denommee et al.*, 2014]. (e) Event bed frequency at Laguna Playa Grande, Vieques [*Donnelly and Woodruff*, 2007]. (f) MDR SST anomaly reconstruction (purple) with 95% uncertainty envelope (gray) [*Mann et al.*, 2009]. NOAA ERSST MDR SST data for 1870–2006 (black) [*Mann et al.*, 2009]. (g) Smoothed modern annual Atlantic tropical cyclone counts (red) and statistical model estimates of basin-wide tropical cyclone counts from 500–1850 C.E. (blue) [*Mann et al.*, 2009]. (h) Ti record from Cariaco Basin sediments thought to reflect changes in terrestrial runoff and the position of the ITCZ [*Haug et al.*, 2001]. Gray shading is interval between 250 and 1150 C.E. when all sites have heightened intense-hurricane–related event beds. Diagonal gray shading is interval between 1150 and 1400 C.E. when Caribbean and GoM sites have heightened intense-hurricane–related event beds and the North American east coast is inactive. Beige shading is interval between 1400 and 1675 C.E. when only the North American east coast is active (Figure 3).
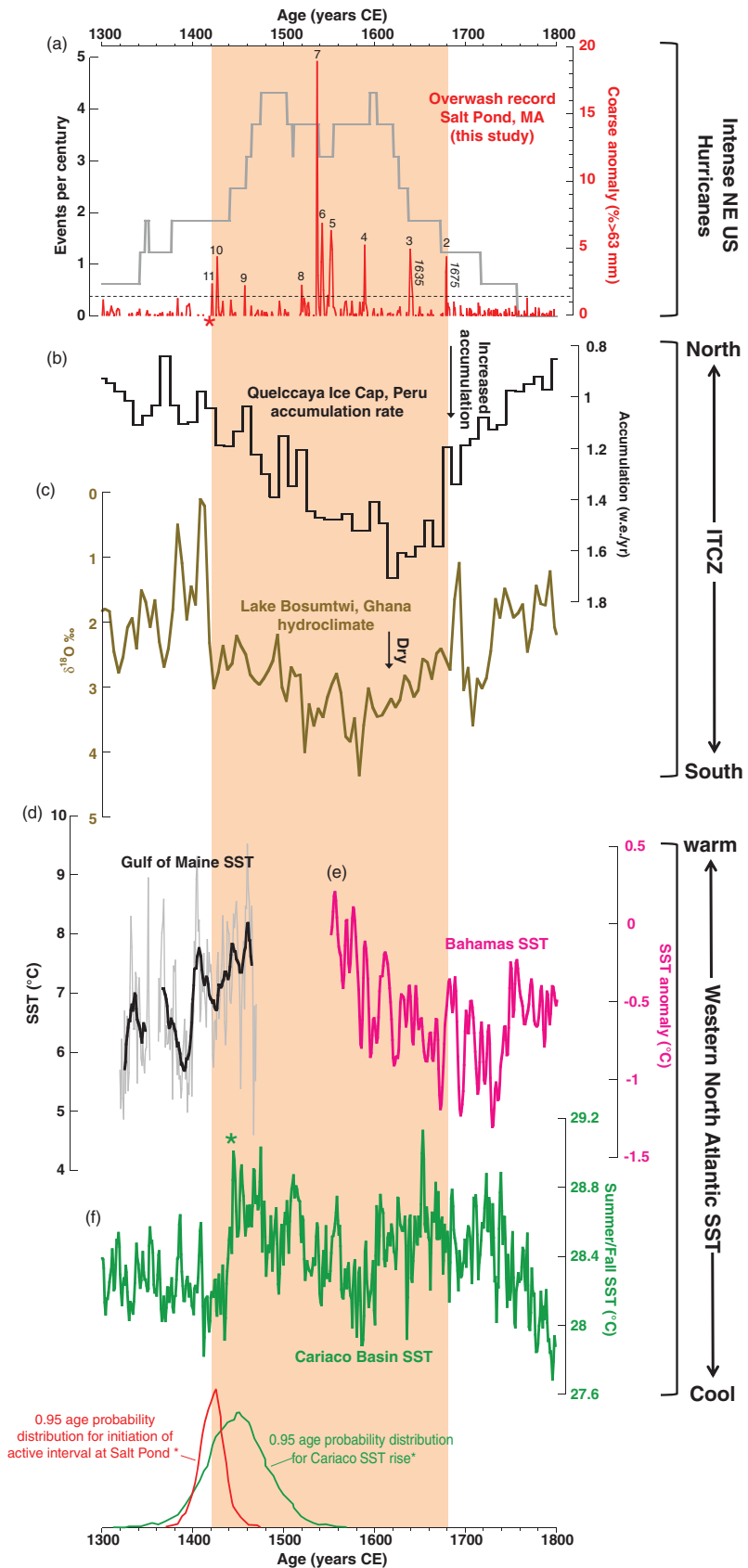
Figure 5. Legend on next page

intense-hurricane activity across much of the western North Atlantic basin between ca. 250 and 1400 C.E. (Figures 4b–4e). ITCZ proxy records also show very similar variability over this time as well. For example, sedimentary Ti influx into the Cariaco Basin has been interpreted as a terrestrial runoff proxy and used to infer past changes in ITCZ position [*Haug et al.*, 2001] (Figure 4h). Higher levels of Ti are thought to represent more terrestrial runoff from increased precipitation in Venezuela from a more northerly mean position of the ITCZ. The Cariaco Basin Ti record closely mirrors the M09 MDR SST reconstruction, which provides further support for a close correspondence between MDR SST and ITCZ position over the last few millennia.

The lack of evidence of intense-hurricane activity along the east coast between 1150 and 1400 C.E., when sites in the Caribbean and GoM remain active (Figure 4), suggests that the trajectory of storms may have shifted away from this region. Alternatively or concurrently, conditions may have been unfavorable for hurricanes to make landfalls at sufficient intensities to leave a geological record of their occurrence. In fact, relatively cool SST off the east coast between 1150 and 1400 C.E. [*Cronin et al.*, 2010; *Keigwin*, 1996; *Wanamaker et al.*, 2008] may have limited hurricane potential intensity, reducing intense-hurricane activity there while the Caribbean and GoM remained active. Alternatively, or in combination with relatively cool SSTs off the east coast, more southerly storm genesis and/or more westerly storm trajectories may have limited intense-hurricane activity along the east coast at this time.

The reorganization of atmospheric and oceanic circulation at the transition from the Medieval Climate Anomaly to the Little Ice Age [*Haug et al.*, 2001; *Kreutz et al.*, 1997], around 1400 C.E., brought cooler MDR SST and a more southerly ITCZ (Figure 4h), resulting in conditions much less favorable for intense-hurricane activity generated in the MDR. Correspondingly, the M09 statistical modeling of basin-wide activity predicts relatively quiescent conditions should have prevailed (Figure 4g) [*Mann et al.*, 2009], and indeed reconstructions from the Caribbean and GoM show a dramatic decrease in event beds at this time. Yet paradoxically, the east coast becomes active at this time based on evidence of increased frequency of intense-hurricane landfalls from The Bahamas to New England between 1420 and 1675 C.E. (Figure 3).

Regional oceanic conditions and/or shifting genesis locations may have played an important role in facilitating intense-hurricane activity along the east coast between 1420 and 1675 C.E., when for example 10 events (#2–11) are recorded at Salt Pond (Figure 5a). Hydroclimate proxies from around the tropical Atlantic indicate a significant shift in tropical precipitation that suggest a southward shift in the ITCZ [*Haug et al.*, 2001], at this time, with drought evident in the tropical northern hemisphere [e.g., *Hodell et al.*, 2005; *Shanahan et al.*, 2009] and increased precipitation in the tropical southern hemisphere [e.g., *Bird et al.*, 2011; *Thompson et al.*, 2013]. In the annually constrained archives from Lake Bostumtwi, Ghana [*Shanahan et al.*, 2009] and the Quelccaya Ice Cap, Peru [*Thompson et al.*, 2013] the hydroclimate changes consistent with a more southerly ITCZ also initiated close to 1420 C.E. and persisted until the late seventeenth century (Figures 5b and 5c). Examining high-resolution SST reconstructions available from the western North Atlantic margin (Figures 5d–5f) reveals that much of this interval is also one of relatively warm SST along the east coast. A Gulf of Maine reconstruction [*Wanamaker et al.*, 2008] appears to capture the onset of this warm SST anomaly indicating a rapid approximately 2°C increase around 1400 C.E. (Figure 5b), which they attribute to increased influence of the Gulf Stream. However, reservoir age uncertainties currently hamper precisely dating this floating chronology [*Wanamaker et al.*, 2013]. An annually dated Bahamian coral-derived temperature reconstruction dating back to 1550 C.E. [*Saenger et al.*, 2009] captures a warm interval and the subsequent cooling (Figure 5e). Reconstructed summer/fall SSTs from the Cariaco Basin

Figure 5. Climatic drivers of increased east coast intense-hurricane activity between 1400 and 1675 C.E. (a) Salt Pond events and event frequency (same as Figure 3a) for the interval 1300–1800 C.E. Shaded area is interval with ten event beds from 1420 to 1675 C.E. (b) Accumulation rate (decadal average; meters of water equivalent per year (m.w.e./yr)) of the Quelccaya Ice Cap in Peru [*Thompson et al.*, 2013]. (c) δ^{18}O-derived lake level proxy (5 year average) from Lake Bosumtwi in West Africa [*Shanahan et al.*, 2009]. (d) δ^{18}O-based SST reconstruction from three *Arctica islandica* samples from the Gulf of Maine (annual data in gray; 11 year moving average in black) [*Wanamaker et al.*, 2008]. (e) Coral-based SST reconstruction from the Bahamas [*Saenger et al.*, 2009]. (f) Mg/Ca-derived *Globigerinoides ruber* summer/fall SST reconstruction from the Cariaco Basin [*Wurtzel et al.*, 2013]. 95% probability distributions (bottom) for the initiation of the active interval at Salt Pond ca. 1420 C.E. (red) and the rise in summer/fall SST in the Cariaco Basin (green). Asterisks (red for Salt Pond; green for Cariaco Basin) indicate interval that relates to the age probability distribution shown.

[*Wurtzel et al.*, 2013] also capture a warm excursion at this time, though here it persists into the eighteenth century (Figure 5f). Comparing the probability distributions (95% confidence) of the onset of the active hurricane interval at Salt Pond with that of the onset of warmer summer/fall SSTs in the Cariaco Basin archive indicates that they may be nearly synchronous within age uncertainties (Figure 5).

SST warming at approximately this time is also evident in more coarsely resolved and poorly dated SST records from the Bermuda Rise [*Keigwin*, 1996] and Chesapeake Bay [*Cronin et al.*, 2010] and coincides with increased transport in the upper 100 m of the Florida Current [*Lund et al.*, 2006]. The combination of increased Florida Current transport and a warm SST anomaly along the east coast could be related to an increase in Atlantic meridional overturning circulation (AMOC) at this time. This potential association of AMOC strengthening and a southerly shift in ITCZ is contrary to some model results, which indicate a southerly migration of the ITCZ is associated with AMOC weakening [*Srokosz et al.*, 2012].

In the modern climate, hurricanes that impact only the east coast develop from prior extratropical disturbances off the southeastern coast of the United States in the subtropical western North Atlantic (i.e., tropical transition) [*McTaggart-Cowan et al.*, 2008]. Therefore, paleoclimate conditions that increased tropical transition cyclogenesis could enhance east coast hurricane activity. For example, the southward shift in the ITCZ (Figures 4h, 5b and 5c) [*Thompson et al.*, 2013; *Shanahan et al.*, 2009] at the onset of the Little Ice Age (ca. 1400–1600 C.E.), which is likely the result of high latitude cooling [*Broccoli et al.*, 2006] and expanding northern hemisphere ice cover [*Chiang and Bitz*, 2005; *Miller et al.*, 2012], could have shifted the track of extratropical disturbances southward, and thus facilitated more hurricane genesis via tropical transition. Examining hurricane genesis with the Atlantic Meridional Mode (AMM), which is an index that captures the interannual variability of the ITCZ and MDR SST (Figure 1a), points to increased hurricane genesis off the southeastern U.S. coast during the most negative phase of AMM (more southerly ITCZ and relatively cool MDR SST) [*Kossin and Vimont*, 2007; *Kossin et al.*, 2010]. In addition, high latitude cooling in combination with the warm SST anomaly in the western North Atlantic would have increased meridional temperature gradients and enhanced atmospheric baroclinicity, which in turn could have increased tropical transition cyclogenesis. Over the period of instrumental data, hurricanes forming via tropical transition in this region do not become as intense as their counterparts that form in the MDR [*McTaggart-Cowan et al.*, 2008], but the warm SST event in the western North Atlantic may have contributed to significant intensification of hurricanes forming off eastern North America during the 15th and 16th centuries.

Compared to the 1500 year model prediction of M09, Atlantic hurricane activity increased significantly over the last century (Figure 4g) in association with warming MDR SST. Most of this increase in hurricane activity occurred in the middle decades of the twentieth century and then the last two decades. However, only Thatchpoint, Bahamas (Figure 3b), Mattapoisett Marsh, MA (Figure 3c), and Lighthouse Bluehole, Belize (Figure 4d) provide evidence of an increase in event bed frequency in the twentieth century. The lack of a coherent pattern of increased hurricane activity across sites may reflect the stochastic nature of landfalling hurricanes and the relatively short interval of warm SST in the MDR. More time in the current regime of relatively warm MDR SST and a greater distribution of sedimentary archives of these events are necessary to better evaluate any recent trends in hurricane activity with sedimentary archives.

4. Conclusions and Implications

Our study reveals that periods of frequent intense-hurricane landfalls that exceeded historical levels occurred over the last 2000 years. Many prehistoric hurricane events beds contain more coarse sediment than historical events, which suggests prehistoric events may have also achieved greater intensity relative to historical hurricanes. As a result, risk assessments based solely on historical evidence may significantly underestimate hurricane threats to coastal communities. Centennial-scale shifts in MDR SST and associated migration of the ITCZ played an important role in driving basin-wide changes in intense-hurricane activity. Persistently warm MDR SST drove heightened levels of intense-hurricane activity across much of the western North Atlantic between ca. 250 and 1400 C.E., however activity along the east coast was suppressed between 1150 and 1400 C.E. A shift in intense-hurricane activity from the Caribbean and GoM to the east coast occurred at the onset of the Little Ice Age (ca. 1400 C.E.). The ensuing interval of heightened intense-hurricane activity confined to the east coast between about 1400 and 1675 C.E. may have been driven by a combination of increased tropical transition cyclogenesis and elevated SSTs off the

east coast. While some sediment-based reconstructions point to modest recent increases in hurricane landfalls in the last century when MDR SST has warmed, others like Salt Pond do not. However, the lack of a coherent recent increase in intense-hurricane event beds may simply reflect the stochastic nature of hurricane landfalls and the relatively short period of recent warm MDR SST.

Future anthropogenic warming will likely be focused in the northern hemisphere, and as a result the ITCZ will occupy a more northerly position [*Broecker and Putnam*, 2013], potentially leading to increased hurricane genesis in the MDR [*Kossin and Vimont*, 2007; *Merlis et al.*, 2013]. More cyclogenesis in the MDR will likely also significantly impact influence the intensity of storms impacting the highly populated western North Atlantic margin, as these long-lived storms tend to become more intense. Thus, intervals with historically unprecedented intense-hurricane activity over the past two millennia provide important analogs for evaluating future hurricane risk. AMOC is projected to weaken over the 21st century due in to greenhouse gas warming [*Stocker et al.*, 2013], but natural variability could result in AMOC strengthening at times. Reduced heat transport via AMOC could cool the higher latitude North Atlantic and potentially offset anthropogenic warming and thus limit future intense-hurricane activity off the east coast. Unfortunately, significant uncertainties exist in the future AMOC variability [*Srokosz et al.*, 2012]. From the perspective of the last two millennia, the magnitude of threat of intense-hurricane landfalls along the North American east coast is likely sensitive to SST both in the MDR as well as along the western North Atlantic margin. Our results confirm modern observations [*Emanuel*, 2005; *Goldenberg et al.*, 2001] and theoretical studies [*Emanuel et al.*, 2004] that link increased hurricane activity with intervals of warmer SST, and provide important context for examining projections of future hurricane activity.

References

Bender, M. A., T. R. Knutson, R. E. Tuleya, J. J. Sirutis, G. A. Vecchi, S. T. Garner, and I. M. Held (2010), Modeled impact of anthropogenic warming on the frequency of intense Atlantic hurricanes, *Science*, *327*(5964), 454–458.

Bird, B. W., M. B. Abbott, M. Vuille, D. T. Rodbell, N. D. Stansell, and M. F. Rosenmeier (2011), A 2,300-year-long annually resolved record of the South American summer monsoon from the Peruvian Andes, *Proc. Natl. Acad. Sci. U. S. A.*, *108*(21), 8583–8588.

Blaauw, M., and J. A. Christen (2011), Flexible paleoclimate age-depth models using an autoregressive gamma process, *Bayesian Anal.*, *6*(3), 457–474.

Black, D. E., L. C. Peterson, J. T. Overpeck, A. Kaplan, M. N. Evans, and M. Kashgarian (1999), Eight centuries of North Atlantic Ocean atmosphere variability, *Science*, *286*(5445), 1709–1713.

Boldt, K. V., P. Lane, J. D. Woodruff, and J. P. Donnelly (2010), Calibrating a sedimentary record of overwash from Southeastern New England using modeled historic hurricane surges, *Mar. Geol.*, *275*(1), 127–139.

Boose, E. R., K. E. Chamberlin, and D. R. Foster (2001), Landscape and regional impacts of hurricanes in New England, *Ecol. Monogr.*, *71*(1), 27–48.

Brandon, C. M., J. D. Woodruff, D. Lane, and J. P. Donnelly (2013), Tropical cyclone wind speed constraints from resultant storm surge deposition: A 2500 year reconstruction of hurricane activity from St. Marks, FL, *Geochem. Geophys. Geosyst.*, *14*(8), 2993–3008, doi:10.1002/GGGE.20217.

Broccoli, A. J., K. A. Dahl, and R. J. Stouffer (2006), Response of the ITCZ to Northern Hemisphere cooling, *Geophys. Res. Lett.*, *33*(1), L01702, doi:10.1029/2005GL024546.

Broecker, W. S., and A. E. Putnam (2013), Hydrologic impacts of past shifts of Earth's thermal equator offer insight into those to be produced by fossil fuel CO2, *Proc. Natl. Acad. Sci. U. S. A.*, *110*(42), 16710–16715.

Brown, C. W. (1939), Hurricanes and shore-line changes in Rhode Island, *Geogr. Rev.*, *29*, 416–430.

Cheung, K. F., L. Tang, J. P. Donnelly, E. M. Scileppi, K. B. Liu, X. Z. Mao, S. H. Houston, and R. J. Murnane (2007), Numerical modeling and field evidence of coastal overwash in southern New England from Hurricane Bob and implications for paleotempestology, *J. Geophy. Res. Earth Surf.*, *112*(F3), F03024, doi:10.1029/2006JF000612.

Chiang, J. C., and C. M. Bitz (2005), Influence of high latitude ice cover on the marine Intertropical Convergence Zone, *Clim. Dyn.*, *25*(5), 477–496.

Clark, J. S., and W. A. Patterson III (1985), The development of a tidal marsh: Upland and oceanic influences, *Ecol. Monogr.*, *55*, 189–217.

Cronin, T., K. Hayo, R. C. Thunell, G. S. Dwyer, C. Saenger, and D. Willard (2010), The medieval climate anomaly and little ice age in Chesapeake Bay and The North Atlantic Ocean, *Palaeogeogr. Palaeoclimatol. Palaeoecol.*, *297*(2), 299–310.

Dean, W. E., Jr. (1974), Determination of carbonate and organic matter in calcareous sediments and sedimentary rocks by loss on ignition: Comparison with other methods, *J. Sediment. Res.*, *44*(1), 242–248.

Denommee, K., S. Bentley, and A. Droxler (2014), Climatic controls on hurricane patterns: A 1200-y near-annual record from Lighthouse Reef, Belize, *Scientific Rep. 4*, 3876, doi:10.1038/srep03876.

Donnelly, J. P. (1998), Evidence of late Holocene post-glacial isostatic adjustment in coastal wetland deposits of eastern North America, *Geores. Forum*, *3*, 393–400.

Donnelly, J. P., S. S. Bryant, J. Butler, J. Dowling, L. Fan, N. Hausmann, P. Newby, B. Shuman, J. Stern, and K. Westover (2001), 700 yr sedimentary record of intense hurricane landfalls in southern New England, *Geol. Soc. Am. Bull.*, *113*(6), 714–727.

Donnelly, J. P., and J. D. Woodruff (2007), Intense hurricane activity over the past 5,000 years controlled by El Nino and the West African monsoon, *Nature*, *447*(7143), 465–468.

Dunphy, P. P., and J. E. Dibb (1994), 137Cs gamma-ray detection at Summit, Greenland, *J. Glaciol.*, *40*(134), 87–92.

Emanuel, K. (2005), Increasing destructiveness of tropical cyclones over the past 30 years, *Nature*, *436*(7051), 686–688.

Emanuel, K. (2013), Downscaling CMIP5 climate models shows increased tropical cyclone activity over the 21st century, *Proc. Natl. Acad. Sci. U. S. A.*, *110*(30), 12219–12224.

Emanuel, K., C. DesAutels, C. Holloway, and R. Korty (2004), Environmental control of tropical cyclone intensity, *J. Atmos. Sci.*, *61*(7), 843–858.

Faegri, K., and J. Iverson (1989), *Textbook of Pollen Analysis*, 398 pp., John Wiley & Sons, New York.

Geoffrey, T. (1930), *Suckanesset: Wherein May be Read a History of Falmouth, Massachusetts (1661–1930)*, Falmouth Publishing Co., Falmouth, Mass.

Goldenberg, S. B., C. W. Landsea, A. M. Mestas-Nuñez, and W. M. Gray (2001), The recent increase in Atlantic hurricane activity: Causes and implications, *Science*, *293*(5529), 474–479.

Gray, W. M. (1968), Global view of the origin of tropical disturbances and storms, *Mon. Weather Rev.*, *96*(10), 669–700.

Gray, W. M. (1990), Strong association between West African rainfall and US landfall of intense hurricanes, *Science*, *249*(4974), 1251–1256.

Haug, G. H., K. A. Hughen, D. M. Sigman, L. C. Peterson, and U. Röhl (2001), Southward migration of the Intertropical Convergence Zone through the Holocene, *Science*, *293*(5533), 1304–1308.

Hodell, D. A., M. Brenner, J. H. Curtis, R. Medina-González, E. Ildefonso-Chan Can, A. Albornaz-Pat, and T. P. Guilderson (2005), Climate change on the Yucatan Peninsula during the little ice age, *Quat. Res.*, *63*(2), 109–121.

Keigwin, L. D. (1996), The little ice age and medieval warm period in the Sargasso Sea, *Science*, *274*(5292), 1503–1508.

Knutson, T. R., J. L. McBride, J. Chan, K. Emanuel, G. Holland, C. Landsea, I. Held, J. P. Kossin, A. Srivastava, and M. Sugi (2010), Tropical cyclones and climate change, *Nat. Geosci.*, *3*(3), 157–163.

Kossin, J. P., and D. J. Vimont (2007), A more general framework for understanding Atlantic hurricane variability and trends, *Bull. Am. Meteorol. Soc.*, *88*(11), 1767–1781.

Kossin, J. P., J. A. Knaff, H. I. Berger, D. C. Herndon, T. A. Cram, C. S. Velden, R. J. Murnane, and J. D. Hawkins (2007), Estimating hurricane wind structure in the absence of aircraft reconnaissance, *Weather Forecast.*, *22*(1), 89–101.

Kossin, J. P., S. J. Camargo, and M. Sitkowski (2010), Climate modulation of North Atlantic hurricane tracks, *J. Clim.*, *23*(11), 3057–3076.

Kozar, M. E., M. E. Mann, S. J. Camargo, J. P. Kossin, and J. L. Evans (2012), Stratified statistical models of North Atlantic basin-wide and regional tropical cyclone counts, *J. Geophys. Res. Atmos.*, *117*(D18), D18103, doi:10.1029/2011JD017170.

Kozar, M. E., M. E. Mann, K. A. Emanuel, and J. L. Evans (2013), Long-term variations of North Atlantic tropical cyclone activity downscaled from a coupled model simulation of the last millennium, *J. Geophys. Res. Atmos.*, *118*(24), 13,383–13,392, doi:10.1002/2013JD020380.

Kreutz, K., P. Mayewski, L. Meeker, M. Twickler, S. Whitlow, and I. Pittalwala (1997), Bipolar changes in atmospheric circulation during the Little Ice Age, *Science*, *277*(5330), 1294–1296.

Landsea, C. W., C. Anderson, N. Charles, G. Clark, J. Dunion, J. Fernandez-Partagas, P. Hungerford, C. Neumann, and M. Zimmer (2004), The Atlantic hurricane database re-analysis project: Documentation for the 1851–1910 alterations and additions to the HURDAT database, in *Hurricanes and Typhoons: Past, Present and Future*, edited by R. J. Murnane and Kam-biu Liu, pp. 177–221, Columbia University Press, New York.

Landsea, C. W., B. A. Harper, K. Hoarau, and J. A. Knaff (2006), Climate change. Can we detect trends in extreme tropical cyclones? *Science*, *313*(5786), 452.

Lane, P., J. P. Donnelly, J. D. Woodruff, and A. D. Hawkes (2011), A decadally-resolved paleohurricane record archived in the late Holocene sediments of a Florida sinkhole, *Mar. Geol.*, *287*(1), 14–30.

Lin, N., P. Lane, K. A. Emanuel, R. M. Sullivan, and J. P. Donnelly (2014), Heightened hurricane surge risk in Northwest Florida revealed from climatological-hydrodynamic modeling and paleo-record reconstruction, *J. Geophys. Res. Atmos.*, *119*(14), 8606–8623, doi:10.1002/2014JD021584.

Ludlum, D. M. (1963), *Early American Hurricanes, 1492–1870*, American Meteorological Society, Boston, Mass.

Lund, D. C., J. Lynch-Stieglitz, and W. B. Curry (2006), Gulf Stream density structure and transport during the past millennium, *Nature*, *444*(7119), 601–604.

Mallinson, D. J., C. W. Smith, S. Mahan, S. J. Culver, and K. McDowell (2011), Barrier island response to late Holocene climate events, North Carolina, USA, *Quat. Res.*, *76*(1), 46–57.

Mann, M. E., J. D. Woodruff, J. P. Donnelly, and Z. Zhang (2009), Atlantic hurricanes and climate over the past 1,500 years, *Nature*, *460*(7257), 880–883.

Mayfield, M. (1991), Preliminary Report Hurricane Bob, 16–20 August 1991. *Rep.*, 21 pp., National Hurricane Center, Miami, Fla.

McCaffrey, R. J., and J. Thomson (1980), A record of the accumulation of sediment and trace metals in a Connecticut salt marsh, *Adv. Geophys.*, *22*, 165–236.

McConnell, J. R., G. W. Lamorey, and M. A. Hutterli (2002), A 250-year high-resolution record of Pb flux and crustal enrichment in central Greenland, *Geophys. Res. Lett.*, *29*(23), 45-41–45-44, doi:10.1029/2002GL016016.

McTaggart-Cowan, R., G. D. Deane, L. F. Bosart, C. A. Davis, and T. J. Galarneau Jr. (2008), Climatology of tropical cyclogenesis in the North Atlantic (1948–2004), *Mon. Weather Rev.*, *136*(4), 1284–1304.

Merlis, T. M., M. Zhao, and I. M. Held (2013), The sensitivity of hurricane frequency to ITCZ changes and radiatively forced warming in aquaplanet simulations, *Geophys. Res. Lett.*, *40*(15), 4109–4114, doi:10.1002/GRL.50680.

Miller, G. H., Á. Geirsdóttir, Y. Zhong, D. J. Larsen, B. L. Otto-Bliesner, M. M. Holland, D. A. Bailey, K. A. Refsnider, S. J. Lehman, and J. R. Southon (2012), Abrupt onset of the Little Ice Age triggered by volcanism and sustained by sea-ice/ocean feedbacks, *Geophys. Res. Lett.*, *39*(2), L02708, doi:10.1029/2011GL050168.

Moy, C. M., G. O. Seltzer, D. T. Rodbell, and D. M. Anderson (2002), Variability of El Niño/Southern oscillation activity at millennial timescales during the Holocene epoch, *Nature*, *420*(6912), 162–165.

Reimer, P. J., E. Bard, A. Bayliss, J. W. Beck, P. G. Blackwell, C. B. Ramsey, C. E. Buck, H. Cheng, R. L. Edwards, and M. Friedrich (2013), IntCal13 and Marine13 radiocarbon age calibration curves 0–50,000 years cal BP, *Radiocarbon*, *55*(4), 1869–1887.

Russell, E. W. B., R. B. Davis, R. S. Anderson, T. E. Rhodes, and D. S. Anderson (1993), Recent centuries of vegetational change in the glaciated north-eastern United States, *J. Ecol.*, *81*, 647–664.

Saenger, C., A. L. Cohen, D. W. Oppo, R. B. Halley, and J. E. Carilli (2009), Surface-temperature trends and variability in the low-latitude North Atlantic since 1552, *Nat. Geosci.*, *2*(7), 492–495.

Shanahan, T. M., J. T. Overpeck, K. Anchukaitis, J. W. Beck, J. E. Cole, D. L. Dettman, J. A. Peck, C. A. Scholz, and J. W. King (2009), Atlantic forcing of persistent drought in West Africa, *Science*, *324*(5925), 377–380.

Srokosz, M., M. Baringer, H. Bryden, S. Cunningham, T. Delworth, S. Lozier, J. Marotzke, and R. Sutton (2012), Past, present, and future changes in the Atlantic meridional overturning circulation, *Bull. Am. Meteorol. Soc.*, *93*(11), 1663–1676.

Sumner, H. (1944), The North Atlantic hurricane of September 8–16, 1944, *Mon. Weather Rev.*, *72*(9), 187–189.

Stocker, T., D. Qin, G. Plattner, M. Tignor, S. Allen, J. Boschung, A. Nauels, Y. Xia, V. Bex, and P. Midgley (2013), *IPCC, 2013: Climate Change 2013: The Physical Science Basis. Contribution of Working Group I to the Fifth Assessment Report of the Intergovernmental Panel on Climate Change*, Cambridge Univ. Press, Cambridge, U. K.

Thieler, E. R., T.L. Smith, J.M. Knisel, and D.W. Sampson (2013), Massachusetts shoreline change mapping and analysis project, *2013 Update Rep.*, 42 pp.

Thompson, L., E. Mosley-Thompson, M. Davis, V. Zagorodnov, I. Howat, V. Mikhalenko, and P.-N. Lin (2013), Annually resolved ice core records of tropical climate variability over the past 1800 years, *Science*, *340*(6135), 945–950.

van de Plassche, O., G. Erkens, F. van Vliet, J. Brandsma, K. van der Borg, and A. F. de Jong (2006), Salt-marsh erosion associated with hurricane landfall in southern New England in the fifteenth and seventeenth centuries, *Geology*, *34*(10), 829–832.

van Hengstum, P. J., J. P. Donnelly, M. R. Toomey, N. A. Albury, P. Lane, and B. Kakuk (2013), Heightened hurricane activity on the Little Bahama Bank from 1350 to 1650 AD, *Cont. Shelf Res.*, *86*, 103–115.

Villarini, G., and G. A. Vecchi (2013), Projected increases in North Atlantic tropical cyclone intensity from CMIP5 models, *J. Clim.*, *26*(10), 3231–3240.

Wallace, D. J., J. D. Woodruff, J. B. Anderson, and J. P. Donnelly (2014), Palaeohurricane reconstructions from sedimentary archives along the Gulf of Mexico, Caribbean Sea and western North Atlantic Ocean margins, *Geological Society, London, Special Publications*, *388*, SP388. 312.

Wanamaker, A. D., Jr., K. J. Kreutz, B. R. Schöne, N. Pettigrew, H. W. Borns, D. S. Introne, D. Belknap, K. A. Maasch, and S. Feindel (2008), Coupled North Atlantic slope water forcing on Gulf of Maine temperatures over the past millennium, *Clim. Dyn.*, *31*(2–3), 183–194.

Wanamaker Jr, A. D., E. E. Lower, S. M. Griffin, and K. J. Kreutz (2013), Tracing slope water currents to the Gulf of Maine (northwestern Atlantic) using radiocarbon derived from a multi-century master shell chronology, in *Proceedings of the Third International Sclerochronology Conference*, Caernarfon, North Wales, U. K.

Webster, P. J., G. J. Holland, J. A. Curry, and H.-R. Chang (2005), Changes in tropical cyclone number, duration, and intensity in a warming environment, *Science*, *309*(5742), 1844–1846.

Woodruff, J. D., J. P. Donnelly, K. Emanuel, and P. Lane (2008a), Assessing sedimentary records of paleohurricane activity using modeled hurricane climatology, *Geochem. Geophys.Geosyst.*, *9*(9), Q09V10, doi:10.1029/2008GC002043.

Woodruff, J. D., J. P. Donnelly, D. Mohrig, and W. R. Geyer (2008b), Reconstructing relative flooding intensities responsible for hurricane-induced deposits from Laguna Playa Grande, Vieques, Puerto Rico, *Geology*, *36*(5), 391–394.

Wu, J., and E. A. Boyle (1997), Lead in the western North Atlantic Ocean: Completed response to leaded gasoline phaseout, *Geochim. Cosmochim. Acta*, *61*(15), 3279–3283.

Wurtzel, J. B., D. E. Black, R. C. Thunell, L. C. Peterson, E. J. Tappa, and S. Rahman (2013), Mechanisms of southern Caribbean SST variability over the last two millennia, *Geophys. Res. Lett.*, *40*(22), 5954–5958, doi:10.1002/2013GL058458.

Zhang, R., and T. L. Delworth (2006), Impact of Atlantic multidecadal oscillations on India/Sahel rainfall and Atlantic hurricanes, *Geophys. Res. Lett.*, *33*(17), L17712, doi:10.1029/2006GL026267.

DONNELLY ET AL.

65